THE JOURNAL OF BIOLOGICAL CHEMISTRY VOL. 283, NO. 36, pp. 24571–24583, September 5, 2008

The Poly(ADP-ribose) Polymerase PARP-1 Is Required for Oxidative Stress-induced TRPM2 Activation in Lymphocytes*

Received for publication, April 7, 2008, and in revised form, June 18, 2008 Published, JBC Papers in Press, July 3, 2008, DOI 10.1074/jbc.M802673200

Ben Buelow[‡§], **Yumei Song**[§], **and Andrew M. Scharenberg**[‡§1]

From the [‡]*Departments of Pediatrics and Immunology, University of Washington and* [§]*Division of Immunology, Seattle Children's Hospital Research Institute, Seattle, Washington 98103*

TRPM2 cation channels are widely expressed in the immune system and are thought to play a role in immune cell responses to oxidative stress. Patch clamp analyses suggest that TRPM2 channel activation can occur through a direct action of oxidants on TRPM2 channels or indirectly through the actions of a related group of adenine nucleotide 2nd messengers. However, the contribution of each gating mechanism to oxidative stress-induced TRPM2 activation in lymphocytes remains undefined. To better understand the molecular events leading to TRPM2 activation in lymphocytes, we analyzed oxidative stress-induced turnover of intracellular NAD, the metabolic precursor of adenine nucleotide 2nd messengers implicated in TRPM2 gating, and oxidative stress-induced TRPM2-mediated currents and Ca^{2+} transients in DT40 B cells. TRPM2-dependent Ca^{2+} entry did not influence the extent or time course of oxidative stress-induced turnover of NAD. Furthermore, expression of oxidative stress-activated poly(ADP-ribose) polymerases (PARPs) was required for oxidative stress-induced NAD turnover, TRPM2 currents, and TRPM2-dependent Ca^{2+} transients; no oxidant-induced activation of TRPM2 channels could be detected in PARP-deficient cells. Together, our results suggest that during conditions of oxidative stress in lymphocytes, TRPM2 acts as a downstream effector of the PARP/poly(ADP-ribose) glycohydrolase pathway through PARP-dependent formation of ADP-ribose.

TRPM2 cation channels are widely expressed in the immune system (1) and have been shown to mediate oxidative stress-induced Ca^{2+} signals in neutrophils, microglia, and T lymphocytes (2–8). Patch clamp analyses of TRPM2 gating indicate that TRPM2 channels may be activated through a direct effect of oxidants, or through cytosolic adenine nucleotide 2nd messengers (3, 5, 7, 9–14). The mechanism of direct gating of TRPM2 channels is not known but appears to involve different molecular events than 2nd messenger-mediated TRPM2 gating, as it occurs in mutant TRPM2 channels lacking the C-terminal NUDT9-H domain (13–17). Cytosolic 2nd messenger-induced gating of TRPM2 has been shown to occur through NAD-derived adenine nucleotide 2nd messenger ADP-ribose (ADPR),[2] 2′-*O*-acetylated ADPR, cyclic ADP-ribose (cADPR), and nicotinic acid adenine dinucleotide phosphate (NAADP) (3–5, 7, 10–13, 16, 18, 19) (Fig. 1). The mechanism of ADPR- and 2′-*O*-acetylated ADPR-induced TRPM2 gating involves their binding to a functional cytosolic C-terminal NUDT9-H domain of TRPM2 (11, 12, 20). The gating mechanisms activated by cADPR and NAADP are unknown, although they are likely related to those of ADPR and 2′-*O*-acetylated ADPR, as the effects of all of the adenine nucleotide 2nd messengers are facilitated by cytosolic Ca^{2+} (3, 14, 18, 21–23). Overall, the distinct gating mechanisms described for TRPM2 suggest potentially different signaling roles for TRPM2 in different cell types, with oxidant gating directly leading to increases in cytosolic Ca^{2+}, and the facilitatory effect of Ca^{2+} on adenine nucleotide 2nd messengers operating as a mechanism for coincidence detection of increases in cytosolic Ca^{2+} and the formation of one or more adenine nucleotide 2nd messengers (18).

Despite the significant progress made in identifying TRPM2 gating mechanisms, the relative contributions of the various gating mechanisms to oxidative stress-induced TRPM2 activation in immune cells remain poorly defined. The mechanisms of generation of cytosolic cADPR and NAADP remain obscure, as the two proteins with known capacity to synthesize these compounds, CD38 and BST-1/CD157, are membrane proteins with their enzymatic domains oriented away from the cytosol (24, 25). Consequently, cell-permeable molecular "mimic" antagonists provide the bulk of evidence implicating cADPR and NAADP in intracellular signal transduction mechanisms (*e.g.* 8-bromo-cADPR and related compounds (3, 14)). In light of recent evidence that NAADP and ADPR can activate various forms of purinergic receptors when applied extracellularly (26–31), the possibility that molecular mimic antagonists of adenine nucleotide 2nd messengers are also acting on these receptors is an important issue that remains to be clarified. Although little is known about the pathways contributing to the formation of 2′-*O*-acetylated ADPR, the poly(ADP-ribose) polymerases (PARP)/poly(ADP-ribose) glycohydrolase (PARG) pathway and its downstream product ADPR have been implicated in oxidative stress-induced TRPM2 activation in nonimmunologic cells through the use of small molecule PARP inhibitors (12, 32, 33). However, as these inhibitors act by competing

* The costs of publication of this article were defrayed in part by the payment of page charges. This article must therefore be hereby marked "*advertisement*" in accordance with 18 U.S.C. Section 1734 solely to indicate this fact.

[1] To whom correspondence should be addressed: Depts. of Pediatrics and Immunology, University of Washington and Seattle Children's Hospital Research Institute, Ste. 700, 1900 9th Ave., Seattle, WA 98103, E-mail: andrewms@u.washington.edu.

[2] The abbreviations used are: ADPR, ADP-ribose; PARP, poly(ADP-ribose) polymerase; cADPR, cyclic ADP-ribose; NAADP, nicotinic acid adenine dinucleotide phosphate; MNNG, *N*-methyl-*N*′-nitrosoguanidine; SIRT, sirtuin; PARG, poly(ADP-ribose) glycohydrolase; HA, hemagglutinin; Bicine, *N*,*N*-bis(2-hydroxyethyl)glycine; hPARP, human PARP; pADPR, poly-ADPR; WT, wild type.

with the nicotinamide moiety of NAD for binding to the PARP active site (34, 35), by analogy with observations that small molecule protein kinase inhibitors targeting nucleotide binding influence the activities of multiple protein kinases (36), small molecule PARP-1 inhibitors potentially affect the function of a range of NAD-binding proteins *in vivo*, confounding interpretation of their effects as being solely because of inhibition of PARP-1 activity (34, 35).

To avoid the limitations of pharmacologic approaches, we sought a genetic approach to analyze the biochemical mechanisms of TRPM2 activation in lymphocytes. Based on evidence implicating ADPR in oxidative stress-induced TRPM2 gating in nonimmune contexts (12, 32), we chose to focus our initial studies on defining the role(s) of the PARP/PARG pathway, thought to be a major source of intracellular ADPR. Informative studies of lymphocyte signaling in PARP-1- and PARP-2-deficient mice are complicated by the presence of the overlapping functions of PARP-1 and PARP-2 in single knock-out animals (37, 38) and embryonic lethality in PARP-1/2 double knock-out animals (39). DT40 B cells are an alternative system that supports facile gene targeting and are well validated for studies of lymphocyte signaling and physiology (40–46). As DT40 cells are able to survive in the absence of PARP/PARG pathway function (47), support TRPM2 activation (48), and are developmentally comparable with mature murine B cells shown to express TRPM2 transcripts (1), we chose them as a model genetic system in which to investigate the role of the PARP/PARG pathway in oxidative stress-induced TRPM2 activation in lymphocytes. The results of our investigations suggest that oxidative stress-induced activation of TRPM2 in lymphocytes is directly dependent on activation of the PARP/PARG pathway and consequent formation of the adenine nucleotide 2nd messenger ADPR.

EXPERIMENTAL PROCEDURES

Cell Culture—Wild type DT40 B lymphocytes (DT40 control cells) and DT40 B lymphocytes constitutively expressing wild type TRPM2 (DT40-TRPM2 cell line) were cultured at 37 °C with 5% CO_2 in RPMI 1640 medium (Mediatech Inc.) supplemented with 10% fetal bovine serum (Mediatech Inc.), 2% chicken serum (Invitrogen), 10 units/ml penicillin/streptomycin (Mediatech Inc.), 2 mM glutamine (Mediatech Inc.), and β-mercaptoethanol (50 μM; Sigma). PARP-1-deficient DT40 cells were a generous gift from Shunichi Takeda.

Molecular Biology—The pApuro vector containing TRPM2 with a glycine for serine substitution at position 1367 and hemagglutinin tag under the control of the chicken β-actin promoter was generated previously in our lab (12). Both PARP-1-deficient and WT DT40 cells were transfected with this vector by electroporation and selected in puromycin (0.5 μg/ml, Sigma). Stable transfection of DT40 B lymphocytes was carried out using a Bio-Rad Gene-Pulser electroporation apparatus. Cells (1×10^7/0.5 ml of serum-free medium) were pulsed in 0.4-cm cuvettes with 50 μg of plasmid DNA at 550 V and 25 microfarads. Individual clones were evaluated for TRPM2 expression via whole cell patch clamp (see below), and those demonstrating the highest maximal current flow were used for Fluo-4, perforated patch clamp, and NAD content studies. In addition, the highest TRPM2-expressing PARP-1-deficient DT40 clone was transfected with a pcDNA5/TO vector containing human PARP-1 cDNA (courtesy of Ted Dawson, The Johns Hopkins University Medical School) via electroporation for the reconstitution studies. Clones were selected in hygromycin (2 mg/ml, Calbiochem) and expression levels determined by Western blot. Subsequently, these reconstituted cells were transfected with a modified pcDNA6TR plasmid (Invitrogen) expressing the Tet repressor protein and containing the pcDNA 4/TO Zeocin resistance cassette to produce a DT40 cell line inducibly expressing hPARP-1. Clones were selected in Zeocin (400 μg/ml, Invitrogen)-containing medium and screened via Western blot for both Tet repressor expression as well as hPARP-1 expression in the presence or absence of doxycycline (1 μg/ml). Selected clones were used for further study.

Calcium Imaging—Changes in cytosolic calcium concentration were measured by quantitating changes in fluorescence from the Fluo-4 No Wash dye (Invitrogen). The Fluo-4 No Wash calcium assay kit was obtained from Molecular Probes (Eugene, OR). The assay buffer used for the experiments is Hanks' balanced salt solution (Invitrogen) supplemented with HEPES buffer (Invitrogen). Assay plates used were tissue culture-treated Techno Plastics Products AG clear 96-well microplates (Midwest Scientific). *N*-Methyl-*N*′-nitrosoguanidine (MNNG; Sigma) was stored in DMSO at 100 mM concentration and kept at −20 °C. Working solutions were prepared fresh from the stock solution on the day of the experiments at a desired final concentration. H_2O_2 (Sigma) was prepared fresh on the day of the experiments at a desired final concentration. GPI-16539 was synthesized and purified as described previously, stored in DMSO at 10 mM concentration, and diluted to the indicated concentrations in assay buffers (73). 2.5×10^5 cells were suspended in 50 μl of Fluo-4 dye and incubated at 37 °C for 30 min, followed by 30 min at room temperature in a single well of a 96-well plate. The fluorescence measurements in DT40 B cells in 96-well plates loaded with Fluo-4 No Wash were performed on the Wallac VICTOR3 fluorescence microplate reader equipped with an injector (PerkinElmer Life Sciences). MNNG and H_2O_2 were prepared in assay buffer at the desired concentration for each of them. MNNG or H_2O_2 (50 μl) was added via the injector to individual wells. The excitation/emission filter pair 485/535 nm was used in the experiments, with 0.1-s measuring time per data point. The injector speed was set at 5. The reading was repeated 60 times.

Whole Cell Patch Clamp—DT40 cells were adhered to glass coverslips by a 10-min incubation in serum-free media and then stored in standard media (see above) until transferred to the extracellular solution (145 mM NaCl, 2.8 mM KCl, 10 mM CsCl, 1 mM $CaCl_2$, 2 mM $MgCl_2$, 10 mM glucose, 10 mM HEPES, pH 7.4). Patch clamp experiments were carried out using a Zeiss Axiovert microscope, equipped with Eppendorf micromanipulators and stage control. Patch clamp recordings were taken using an EPC9 amplifier (Heka) and a G4 Macintosh computer. Cells were patched with borosilicate glass pipettes pulled with a Sutter instruments P-97 micropipette puller: pipettes had 3-megohm tips. Pipettes were filled with intracellular solution containing 145 mM cesium glutamate, 8 mM NaCl, 1 mM $MgCl_2$, and 10 mM HEPES, pH 7.4, with or without

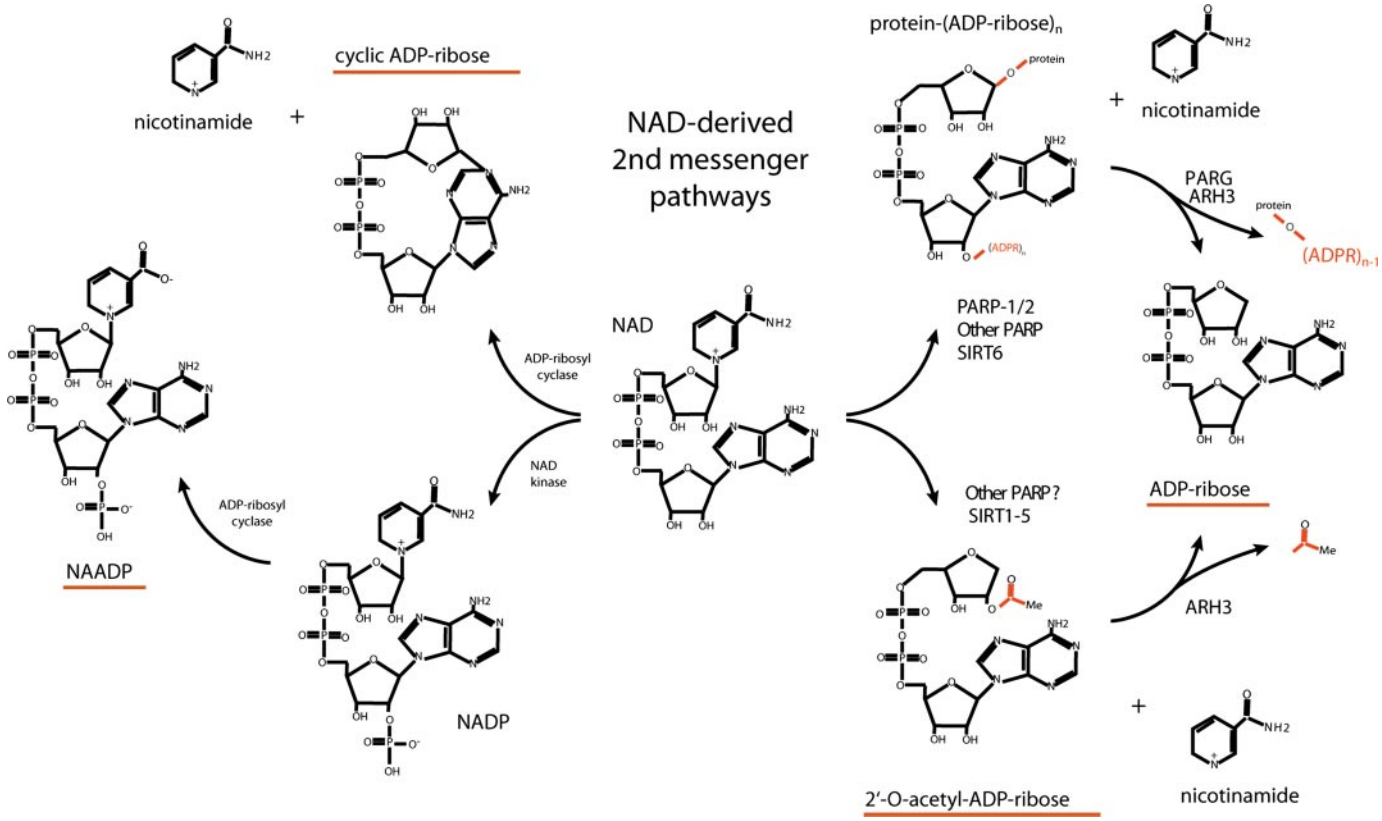

FIGURE 1. **Schematic of pathways leading to adenine nucleotide 2nd messenger production.** Metabolic labeling studies indicate that NAD is turned over solely through hydrolysis of the glycosidic nicotinamide-ribose bond. Two major intracellular mechanisms are known to involve hydrolysis of the nicotinamide moiety from NAD as follows: protein ADP-ribosylation, which is mediated by members of the PARP family as well as several members of the sirtuin (SIRT) protein family, and NAD-dependent protein deacetylation, which at present is thought to be mediated solely by members of the SIRT protein family. Following hydrolysis of the nicotinamide moiety from NAD, both mechanisms require an additional enzymatic step to form ADPR. In the former case, ADPR adducts are released as ADPR in deribosylation reactions catalyzed by PARG or ARH3 (ADP-ribose protein hydrolases 3); in the latter case, 2′-*O*-acetylated ADPR may be deacetylated by ARH3 or other as yet undefined ADPR deacetylases (75, 76). NAD may also be turned over in a similar manner by CD38 and its close homologue BST-1, resulting in the production of ADPR or cADPR, which is subsequently thought to be metabolized to ADPR. Finally, phosphorylation of NAD to NADP allows the possibility for formation of NAADP by CD38/BST-1 at low pH (77). Accumulating information implicates ADP-ribosylation/deribosylation and protein deacetylation in myriad cell physiological processes (38, 52, 66, 78, 79). PARP family ADP-ribosyltransferases have been implicated in DNA repair and transcription (PARP-1/PARP-2 (reviewed in Refs. 37, 38, 52)), spindle structure formation, and telomere maintenance (tankyrase-1 and tankyrase-2 (80–84)), STAT6-dependent transcriptional regulation (CoaSt6 (85, 86)), and transcriptional regulation of as yet undefined genes (BAL-2/3 (87)). In addition, six SIRT family proteins with documented ADPR transferase or protein deacetylase enzymatic activities have been implicated in protein deacetylation linked to metabolic and receptor-mediated signals (SIRT1 and SIRT2 (88–93)), regulation of mitochondrial metabolism, and nuclear-mitochondrial signaling (SIRT3–5, with the role of SIRT4 in regulation of mitochondrial metabolism being secondarily linked to insulin secretion in pancreatic beta cells (94–104)), and chromosomal instability and aging (SIRT6 (105, 106)).

100 μM ADPR. Following formation of a gigaseal, the membrane patch was ruptured by suction, and recordings were taken for 300 s. 50-ms voltage ramps were run every 2 s from −100 to +100 mV. Data analysis was performed using Pulse software, and plots were generated using IgorPro.

Perforated Patch Clamp—All methods were identical to those described above under "Whole Cell Patch Clamp" except the following. No ADPR or ATP was included in the intracellular solution; instead, 240 μg/ml of amphotericin B were included. After formation of the gigaseal, recordings were taken for 2000 s with voltage ramps identical to those above. Subsequently, MNNG was added to the bath solution for a final concentration of 500 μM MNNG, and recordings were taken for a further 2000 s. Cells in which abrupt current jumps occurred, or in which current magnitudes exceeded average whole cell currents observed for that cell line, were excluded from final analyses.

NAD Assay—The NAD assay was performed according to the method of Jacobson and Jacobson (74) with minor modifications. Briefly, 1×10^6 cells were resuspended in 290 μl of media in a single well of a 96-well plate. Wells received 10 μl of 3 mM MNNG or H_2O_2 (for a final concentration of 100 μM) at 5-min intervals over a total time course of 30 min (three wells per time point). Cells were pelleted at 1500 rpm for 5 min and lysed in 100 μl of 0.5 N $HClO_4$ for 15 min on ice and in the dark. Cellular debris was removed by centrifugation at 1500 × *g* for 10 min. On ice and in the dark, 100 μl of KOH and 100 μl of K_2HPO_4/KH_2PO_4, pH 7.2, were added to the supernatant and incubated for 15 min. The $KClO_4$ precipitate was removed via centrifugation at 1500 × *g* for 10 min. 25 μl of the supernatant was incubated for 5 min at 37 °C with 2 mM phenazine ethosulfate, 0.5 mM 3-(4,5-dimethylthiazol-2-yl)-2,5-diphenyltetrazolium bromide, 50 mM EDTA, 600 mM ethanol, and 120 mM Bicine, pH 7.8. 12.5 μl of alcohol dehydrogenase (1 mg/ml, Sigma) were added, and the plate was incubated for a further 20 min at 37 °C. The plate was then read for 1 s/well using a VICTOR3 plate reader at 570 nm. Data analysis was performed in Microsoft Excel and Igor Pro. Fluctuations

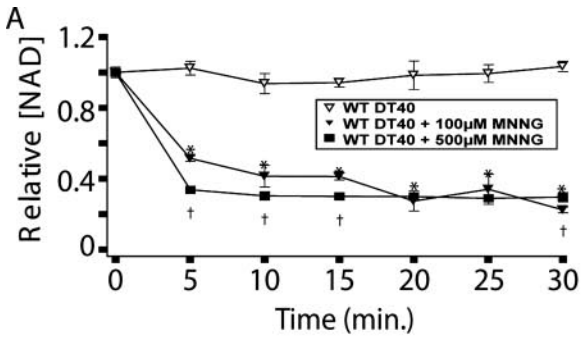
A
Relative [NAD]
1.2
0.8
0.4
0
WT DT40
WT DT40 + 100μM MNNG
WT DT40 + 500μM MNNG
0 5 10 15 20 25 30
Time (min.)

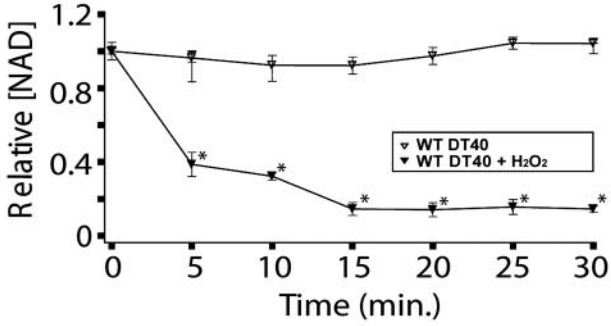
Relative [NAD]
1.2
0.8
0.4
0
WT DT40
WT DT40 + H2O2
0 5 10 15 20 25 30
Time (min.)

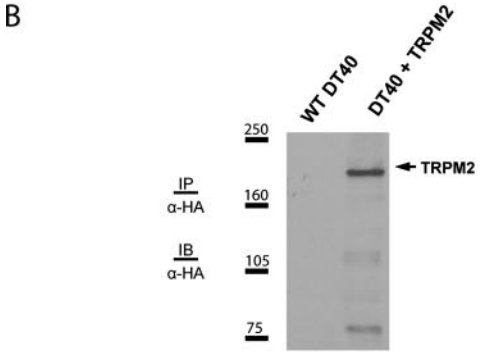
B
WT DT40
DT40 + TRPM2
250
160
105
75
IP
α-HA
IB
α-HA
TRPM2

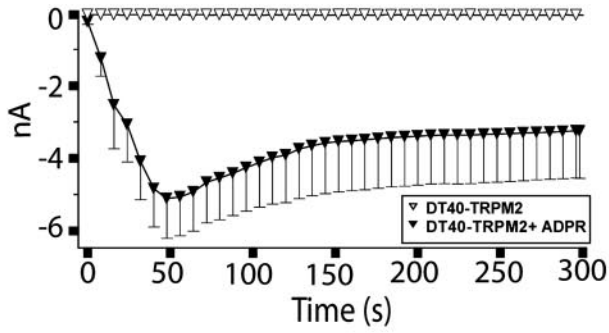
nA
0
-2
-4
-6
DT40-TRPM2
DT40-TRPM2+ ADPR
0 50 100 150 200 250 300
Time (s)

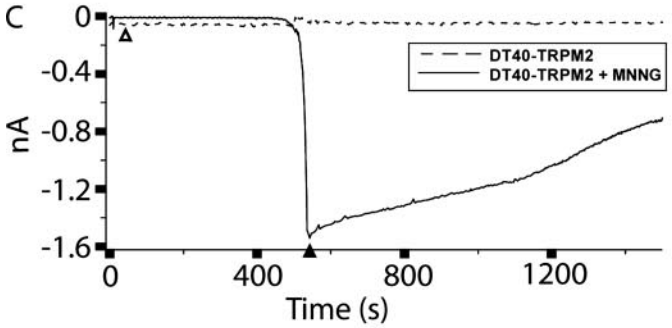
C
nA
0
-0.4
-0.8
-1.2
-1.6
DT40-TRPM2
DT40-TRPM2 + MNNG
0 400 800 1200
Time (s)

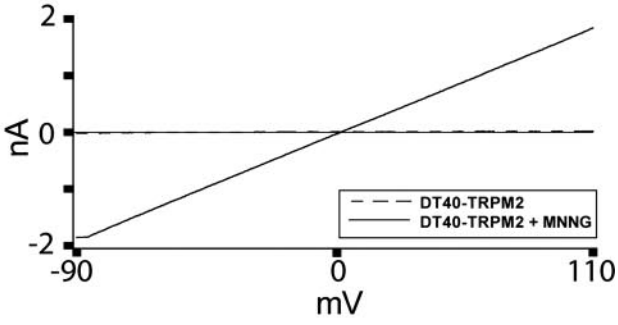
nA
2
0
-2
DT40-TRPM2
DT40-TRPM2 + MNNG
-90 0 110
mV

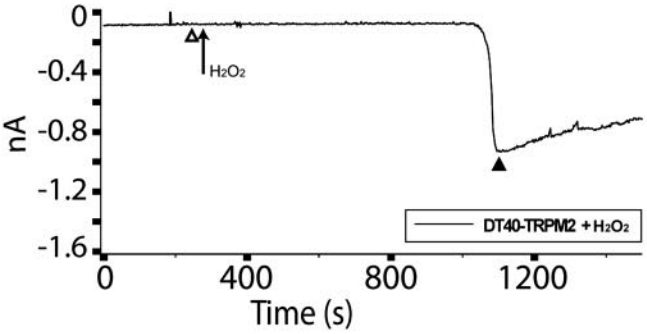
nA
0
-0.4
-0.8
-1.2
-1.6
H2O2
DT40-TRPM2 + H2O2
0 400 800 1200
Time (s)

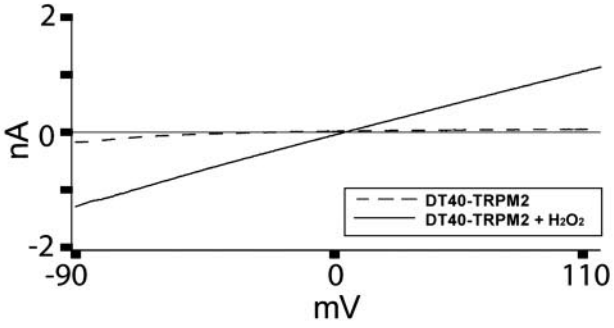
nA
2
0
-2
DT40-TRPM2
DT40-TRPM2 + H2O2
-90 0 110
mV

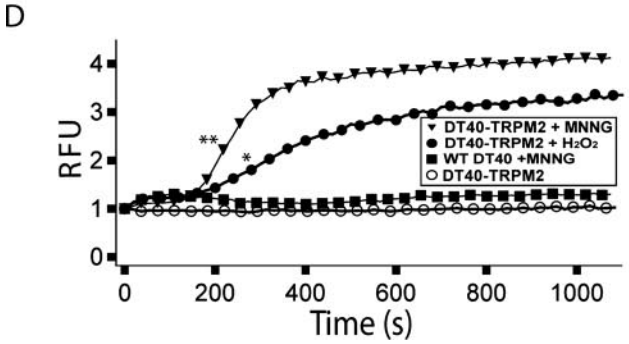
D
RFU
4
3
2
1
0
DT40-TRPM2 + MNNG
DT40-TRPM2 + H2O2
WT DT40 +MNNG
DT40-TRPM2
0 200 400 600 800 1000
Time (s)

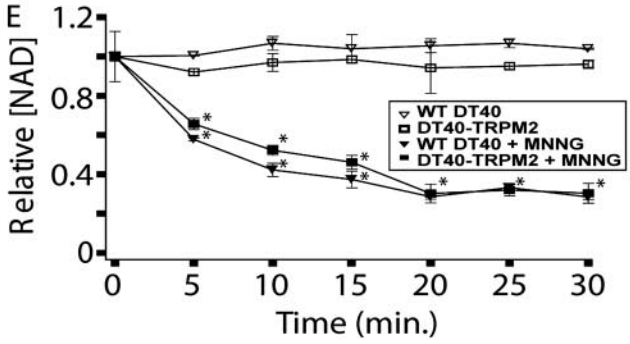
E
Relative [NAD]
1.2
0.8
0.4
0
WT DT40
DT40-TRPM2
WT DT40 + MNNG
DT40-TRPM2 + MNNG
0 5 10 15 20 25 30
Time (min.)

among untreated series from all cell lines between 80 and 120% of base line were observed, which were judged to lack practical relevance. To control for these, a conservative statistical significance level of $p \leq 0.001$ was chosen, as deviations from base line in untreated controls in individual plates did not reach statistical significance by this criterion.

Western Blotting—Western blotting was performed in 6–12% acrylamide (29:1) SDS-polyacrylamide gels. Immunoprecipitation of HA-TRPM2 was done on 500 μg of protein from relevant cell lines incubated with HA antibody (1:100, Cell Signaling) overnight and precipitated using protein G beads. The following primary antibodies were used for blotting: monoclonal anti-HA (1:1000, Cell Signaling) and polyclonal rabbit anti-human PARP-1 (1:4000, Alexis Biochemicals). Note that this antibody cross-reacts with chicken PARP-1 and can be used to evaluate chicken PARP-1 expression between DT40 cell lines. However, as it is polyclonal, it cannot be used to compare chicken PARP-1 levels with transfected human PARP-1. Secondary antibodies were peroxidase-conjugated donkey anti-rabbit and sheep anti-mouse from Amersham Biosciences (1:10,000). Visualization was performed using the ECL reagents from Amersham Biosciences.

RESULTS

DT40 B Cells Phenocopy Oxidative Stress-induced NAD Turnover Observed in Murine and Human Lymphocytes—As NAD is a direct upstream substrate of adenine nucleotide 2nd messengers implicated in TRPM2 gating, and metabolic studies indicate NAD turnover occurs solely through hydrolysis of the nicotinamide glycosidic bond (49–51) (known mechanisms are outlined in Fig. 1), changes in intracellular NAD levels are an informative surrogate marker for the generation of NAD-derived adenine nucleotide 2nd messengers. Previous work in many vertebrate cell types has shown that the rate of intracellular NAD turnover increases following exposure to oxidative or nitrosative stress, resulting in a decrease in intracellular NAD levels (reviewed in Refs. 37, 38, 52). As an initial evaluation of DT40 cells as a system for the study of oxidative stress-induced responses, we analyzed cellular NAD content before and after application of *N*-methyl-*N*′-nitro-*N*-nitrosoguanidine (MNNG) or H_2O_2 as model nitrosative or oxidative stressors, respectively (53, 54) (Fig. 2*A*). As can be seen, application of MNNG or H_2O_2 resulted in a time- and dose-dependent decrease in intracellular NAD, with levels declining rapidly within 300 s of application of either 500 μM MNNG or 100 μM MNNG or H_2O_2. Thus, DT40 cells exhibit oxidative stress-induced turnover of NAD suggestive of an increased rate of production of adenine nucleotide 2nd messengers.

Oxidative Stress-induced NAD Turnover Is Ca^{2+}-independent and Temporally Correlates with TRPM2-dependent Ca^{2+} Transients—If adenine nucleotide 2nd messengers are involved in TRPM2 gating in lymphocytes, then their production should be temporally consistent with the onset of TRPM2 gating. To evaluate the relationship between TRPM2 activation and oxidative stress-induced NAD turnover, we examined the time courses for oxidative stress-induced TRPM2-mediated currents and Ca^{2+} transients in DT40 cells using DT40 cells stably expressing TRPM2 (DT40-TRPM2 cells). TRPM2 expression in the DT40-TRPM2 cells is demonstrated by Western blotting and whole cell patch clamp in Fig. 2*B*, *left* and *right panels*, respectively. Consistent with NAD turnover leading to production of TRPM2 gating messengers, MNNG and H_2O_2 induced large currents in DT40-TRPM2 cells that were absent in WT DT40 cells as measured by perforated patch clamp (Fig. 2*C*). That the currents depended on NAD turnover and consequent adenine nucleotide messenger production for TRPM2 gating is supported by our consistent observation of response latencies for current development of >300 s (at which point 50–80% off NAD has turned over, see Fig. 2*A* and also Figs. 2*E*, 3*C*, 4*D*, and 5*C*). One issue with definitive interpretation of current onset response latencies in these experiments is that the bath solution cannot be effectively circulated during perforated patch recordings used to monitor the currents. Thus, the time between addition of MNNG or H_2O_2 to the bath and when they reached an effective concentration at the cells contributes to the observed response latency for current development. As an additional means to correlate TRPM2 activation with NAD turnover, TRPM2-dependent Ca^{2+} transients were monitored after application of 500 μM MNNG or H_2O_2. As the Ca^{2+} transients are monitored under conditions where bath mixing occurs, the times to effective concentration of the MNNG and H_2O_2 are essentially instantaneous, allowing a more definitive interpretation of the response latencies. Increases in cytoplasmic Ca^{2+}

FIGURE 2. **Wild type DT40 cells support oxidative stress-dependent NAD turnover and TRPM2-dependent Ca^{2+} transients and currents.** *A,* NAD turnover in WT DT40 cells following application of either 500 μM MNNG or 100 μM MNNG or H_2O_2. WT DT40 cells were analyzed for NAD content before and after application of 100 or 500 μM MNNG, as indicated. *Asterisks* indicate a *p* value of ≤0.001 as compared with the untreated controls. *Daggers* indicate a *p* value of ≤0.03 as compared with WT DT40 + 100 μM MNNG at the same time point. *B,* TRPM2 expression in DT40-TRPM2 cells. *Left panel,* WT DT40 cells stably expressing TRPM2 (DT40-TRPM2 cells) were generated as described under "Experimental Procedures." HA-tagged TRPM2 was immunoprecipitated (*IP*) with mouse anti-HA antibody from 500 μg of DT40-TRPM2 protein extract, and the immunoprecipitates were analyzed by Western immunoblotting (*IB*) using anti-HA antibody. *Right panel,* DT40-TRPM2 cells show ADPR-dependent currents by whole cell patch clamp. DT40-TRPM2 cells were patched in the whole cell configuration; the pipette contained IC solution with or without 100 μM ADPR, as indicated. No current was detected in the absence of ADPR, but when the pipette solution contained 100 μM ADPR, ~5 nA of current developed within 50 s, followed by an extended plateau. I/V curves were linear, as is characteristic of TRPM2. *C,* DT40-TRPM2 cells show oxidative stress-induced linear currents. Following establishment of the perforated patch configuration, control recordings were taken from a patched cell (the *dashed line* shows a representative trace) for 1000 sweeps (~30 min). Subsequently, MNNG (*top panels*) or H_2O_2 (*bottom panels*) was added to the bath solution to a final concentration of 500 μM, and recordings were taken for another 1000 sweeps (the *solid line* shows a representative trace). In the H_2O_2 trace shown, the control and treatment I/V curves were taken from the same series of sweeps, before and after application of H_2O_2, respectively. I/V curves from sweeps recorded during the control series (*open triangle*) and the treatment series (*closed triangle*) are shown in the *right panels*. *D,* DT40-TRPM2 cells exhibit oxidative stress-induced Ca^{2+} transients. Intracellular Ca^{2+} was analyzed by Fluo-4 in DT40-TRPM2 cells without and with application of 500 μM MNNG or H_2O_2, as indicated. The *asterisk* indicates a *p* value of ≤0.05 from WT DT40 + MNNG. The *double asterisk* indicates a *p* value of ≤0.003 from WT DT40 + MNNG. For both MNNG and H_2O_2 all subsequent points have a *p* value satisfying these criteria. *E,* TRPM2 expression does not affect NAD turnover. NAD turnover in WT DT40 and DT40-TRPM2 cells was analyzed as in *A* in the absence or presence of 100 μM MNNG, as indicated. *Asterisks* indicate a *p* value of ≤0.001 as compared with the untreated controls.

occurred with a response latency of ~300 s in the DT40-TRPM2 cells (Fig. 2*D*). That the observed Ca^{2+} transients are because of TRPM2 gating is supported by absent (MNNG) or very small (H_2O_2) Ca^{2+} transients in WT DT40 cells lacking TRPM2 expression (Fig. 2*D*; note that H_2O_2 is known to activate phospholipase Cγ-mediated calcium release in DT40 cells, accounting for the small TRPM2-independent Ca^{2+} transient (55)). Overall, TRPM2 activation, as monitored by elevation of cytosolic Ca^{2+}, corresponds well with the time course for turnover of NAD observed after application of 500 μM MNNG or H_2O_2 (as noted above, see Fig. 2, *A* and *E*, and Figs. 3*C*, 4*D*, and 5*C*), supporting the hypothesis that a causal relationship exists between NAD turnover (with consequent adenine nucleotide 2nd messenger production) and TRPM2 gating.

A potential confounding factor in determining the influence of endogenously produced adenine nucleotide 2nd messengers on TRPM2 gating is that TRPM2-mediated Ca^{2+} entry may influence biochemical pathways leading to adenine nucleotide

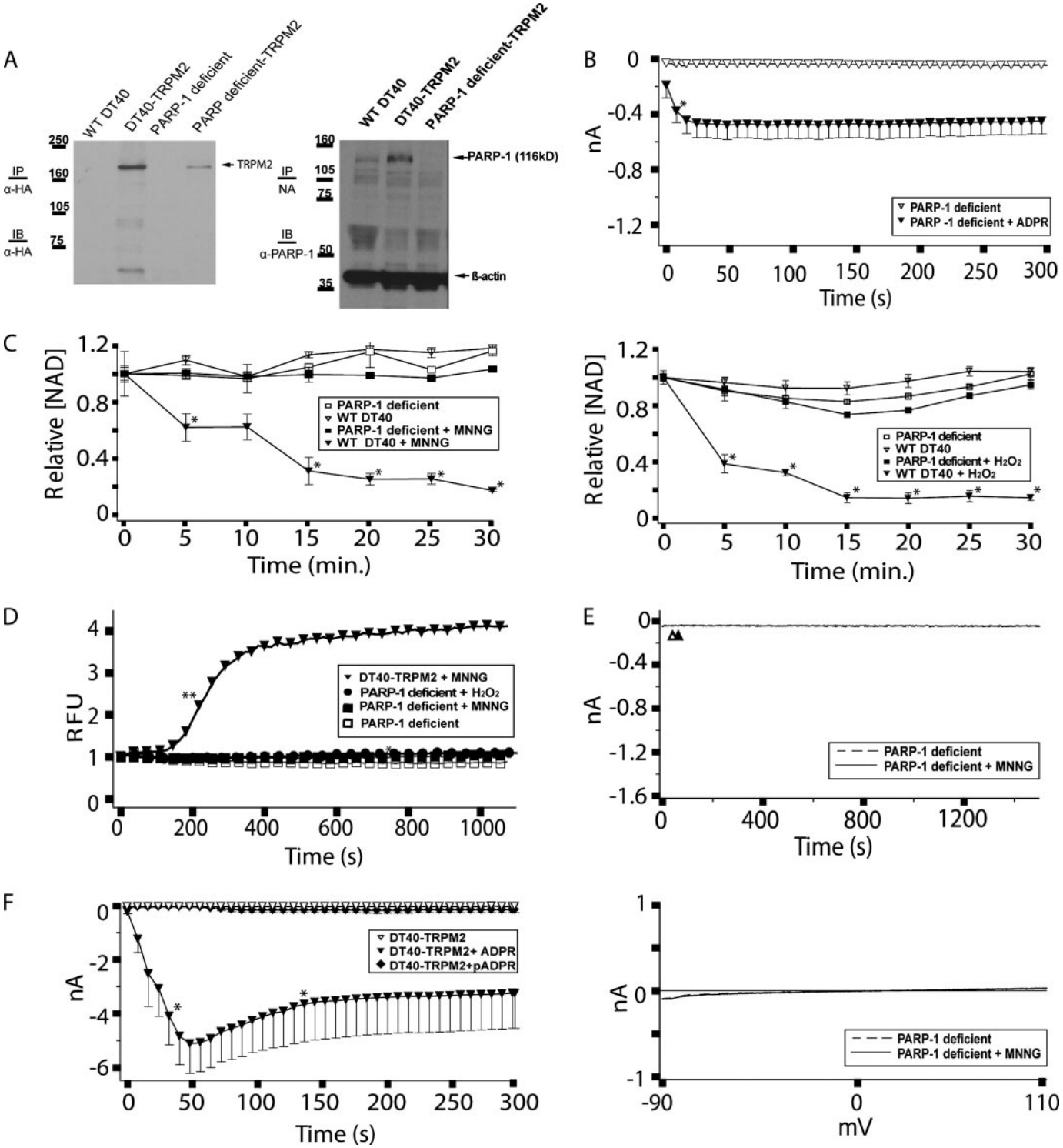

2nd messenger production (*e.g.* PARP-1 (56, 57)). To control for this, we compared NAD turnover in the presence and absence of TRPM2 over a period of 30 min after application of 100 μM MNNG (Fig. 2*E*). For these experiments, an MNNG concentration of 100 μM was used based on the rationale that it would allow a better resolution of differences in the rate of NAD turnover between the various cell lines than application of 500 μM MNNG. Despite a slightly higher level of PARP expression in the DT40-TRPM2 cells (Fig. 3*A*), the WT DT40 cells and the DT40-TRPM2 cells exhibited very similar time courses of NAD degradation, exhibiting loss of ~50% of their NAD content within 300 s in response to 100 μM MNNG. Overall, the similar curves for NAD degradation in WT DT40 and DT40-TRPM2 cells indicate that TRPM2-mediated Ca^{2+} entry does not alter the rate of oxidative stress-induced NAD turnover in DT40 cells in response to MNNG, consistent with previous results (107).

Loss of PARP abrogates oxidative stress-induced NAD degradation and TRPM2-dependent calcium transients and currents in DT40 cells. Overall, the above data are most consistent with the hypothesis that TRPM2 activation in lymphocytes lies downstream from the molecular events responsible for oxidative stress-induced NAD turnover and production of adenine nucleotide 2nd messengers. Genetic approaches have implicated both PARP-1 and PARP-2 in oxidative stress-induced turnover of NAD in murine and human systems, and partial reductions of NAD turnover are observed with each single knock-out (see Refs. 37, 52). However, embryonic lethality of PARP-1/PARP-2 double knock-outs has prohibited analysis of lymphocyte responses in the complete absence of PARP/PARG pathway signaling, and no studies have evaluated TRPM2 activation in single knock-out PARP-deficient lymphocytes. As mentioned above, DT40 cells lack native PARP-2, and viable PARP-1-deficient DT40 cells have been generated (47); thus their use allows an unambiguous analysis of the role of the PARP/PARG pathway in oxidative stress-induced TRPM2 activation.

To generate a system for study of TRPM2 activation in a PARP-deficient context, we transfected PARP-1-deficient DT40 cells with a eukaryotic expression construct driving expression of TRPM2 and isolated individual stable clones. TRPM2 expression in a panel of clones was evaluated by Western blotting and whole cell patch clamp, and the clone with the highest level of TRPM2 expression (based on the whole cell current magnitude) was chosen for further analysis (these cells were designated the "PARP-deficient TRPM2" cell line, Fig. 3, *A* and *B*). Using the PARP-deficient TRPM2 cells, we evaluated NAD turnover in comparison with DT40-TRPM2 cells (Fig. 3*C*), and we observed a complete absence of MNNG- or H_2O_2-induced NAD turnover over the 30-min assay period in the PARP-deficient TRPM2 cells. Furthermore, extension of the time course of observation out to 2 h revealed no apparent decrease in the NAD content of the PARP-deficient TRPM2 cells (data not shown). These results indicate that in DT40 cells, PARP-1 is absolutely required for oxidative stress-induced NAD turnover.

We next evaluated the PARP-deficient TRPM2 cell line using a Fluo-4 Ca^{2+} assay (Fig. 3*D*) and perforated patch clamp (Fig. 3*E*). Consistent with the lack of NAD turnover, we observed a complete absence of any MNNG-activated Ca^{2+} transients or TRPM2-dependent currents. Similar experiments using H_2O_2 to induce NAD turnover and Ca^{2+} transients also showed a complete absence of NAD turnover and only the small TRPM2-independent cytosolic Ca^{2+} transient in the PARP-deficient TRPM2 cells (Fig. 3, *C* and *D*). We were not able to obtain perforated patch recordings in the PARP-deficient cells with H_2O_2 because of an inability to maintain a high resistance seal in these cells after H_2O_2 application.

The above results clearly demonstrate that expression of an oxidative stress-activated PARP enzyme is required for oxidative stress-induced NAD turnover and TRPM2 activation. As PARP directly produces poly-ADPR (pADPR), which is subsequently degraded to monomeric ADPR by the enzyme PARG, either of these adenine nucleotide messengers could potentially account for the observed PARP-dependent TRPM2 activation. To determine whether either or both ADPR and pADPR were contributing to TRPM2 activation, we compared their ability to generate TRPM2 gating in whole cell patch clamp experiments. Consistent with previous reports, monomeric ADPR is able to rapidly induce TRPM2 gating at a 100 μM concentration. However, pADPR at the same concentration did not induce any detectable TRPM2 gating (Fig. 3*F*). These results suggest that

FIGURE 3. **PARP-deficient DT40 cells do not support oxidative stress-induced NAD turnover or TRPM2-dependent Ca^{2+} transients and currents.** *A,* expression of TRPM2 and PARP-1 in DT40-TRPM2 and PARP-deficient TRPM2 cells. *Left panel,* HA-tagged TRPM2 was immunoprecipitated (*IP*) with mouse anti-HA antibody from 500 μg of protein extracted from each of the indicated cell types. The immunoprecipitates were then analyzed by Western immunoblotting (*IB*) with the same antibody. Note: *1st two lanes* of this gel are the same as in Fig. 2*A* and are provided for comparison purposes. *Right panel,* WT and PARP-deficient clones were lysed, and 50 μg of protein was run in each lane of an SDS-polyacrylamide gel. Rabbit anti-human PARP-1 polyclonal antibody was used for immunoblotting of PARP-1. *NA,* not applicable. *B,* PARP-deficient TRPM2 cells exhibit ADPR-dependent currents by whole cell patch clamp. PARP-deficient TRPM2 cells were patched in the whole cell configuration; when the pipette solution contained 100 μM ADPR, ~0.5 nA of current developed within 50 s, followed by an extended plateau characteristic of TRPM2, as indicated. The *asterisk* indicates a p value of $\leq$0.05 from the ADPR-free control recording. All subsequent points also differ from the control with a p value of $\leq$0.05. *C,* NAD turnover is eliminated in PARP-deficient DT40 cells. NAD turnover in the indicated cell lines was assessed as in Fig. 2, *left panel,* MNNG treatment. Fig. 2, *right panel,* H_2O_2 treatment. *Asterisks* indicate a p value of $\leq$0.001 as compared with the untreated controls. Note that the data for DT40 cells in this figure is the same as presented in Fig. 2*A*. *D,* PARP-deficient TRPM2 cells exhibit no oxidative stress-induced Ca^{2+} transients, as indicated. PARP-deficient TRPM2 cells were left untreated, or were treated with 500 μM MNNG or H_2O_2, and intracellular Ca^{2+} was monitored using Fluo-4. *Asterisks* indicate a p value of $\leq$0.05 from DT40-TRPM2. *Double asterisks* indicate a p value of $\leq$0.001 from DT40-TRPM2. For DT40-TRPM2 + MNNG, all subsequent points have a p value of $\leq$0.001. *E,* PARP-deficient TRPM2 cells do not exhibit oxidative stress-induced TRPM2 gating. The experiment was performed as described in Fig. 2*C*, except using PARP-deficient TRPM2 cells. *Top panel,* no MNNG application, *dashed line*; with MNNG application, *solid line*. Sweeps recorded during the control series (*open triangle*) and the treatment series (*closed triangle*) are shown in the *bottom panel*. *F*, DT40-TRPM2 cells show monomeric ADPR-dependent currents by whole cell patch clamp. DT40-TRPM2 cells were patched in the whole cell configuration; the pipette contained IC solution with or without 100 μM ADPR or pADPR, as indicated. No current was detected in the absence of ADPR, but when the pipette solution contained 100 μM ADPR, ~5 nA of current developed within 50 s, followed by an extended plateau. I/V curves were linear, as is characteristic of TRPM2. All points between the *asterisks* differ from the ADPR-free control recording with a p value of $\leq$0.05. Very small or no current was detected following application of 100 μM pADPR.

PARP-mediated NAD turnover leads to eventual PARG-mediated generation of monomeric ADPR, and that accumulation of monomeric ADPR is the dominant means of PARP-dependent activation of TRPM2 channels and TRPM2-dependent Ca^{2+} transients.

Inducible PARP-1 Expression in PARP-deficient DT40 Cells Leads to Doxycycline-dependent Oxidative Stress-induced NAD Degradation and TRPM2-dependent Calcium Transients—Given the well demonstrated role of ADPR in TRPM2 gating (3, 5, 7, 12, 20, 58, 59), the data above suggest a critical involvement of the PARP/PARG pathway in the production of ADPR required for oxidative stress-induced TRPM2 activation in lymphocytes. However, they are subject to the caveat that the PARP-deficient DT40 cells we used have been selected for their capacity to tolerate a complete lack of PARP expression, and thus their responses could reflect an altered ability to respond to oxidative stress. To control for this possibility, we reconstituted the PARP-deficient TRPM2 cells with an inducible human PARP-1 expression construct (designated as "PARP-inducible TRPM2" cells). As can be seen in Fig. 4*A*, this cell line exhibits very little hPARP-1 prior to induction. In addition, PARP-inducible TRPM2 cells demonstrate statistically indistinguishable ADPR-dependent whole cell currents (Fig. 4, *B* and *C*), and immunoprecipitiation Western blotting for TRPM2 protein (Fig. 4*D*) before and after hPARP-1 induction. Parallel analysis of NAD turnover and intracellular Ca^{2+} before and after induction demonstrated absent MNNG- or H_2O_2-induced NAD turnover and absent/reduced intracellular Ca^{2+} prior to induction, and full recovery of both MNNG- or H_2O_2-induced NAD turnover and increased intracellular Ca^{2+} after induction (Fig. 4, *E* and *F,* respectively). As noted previously (60, 61), treatment with H_2O_2 leads to small increases in intracellular Ca^{2+} in the absence of TRPM2 because of phospholipase Cγ2 activation; this accounts for the increased signal in the PARP-inducible TRPM2(−) that partially obscures the TRPM2-dependent effects (Fig. 4*F*). Perforated patch clamp attempts were not successful with either MNNG or H_2O_2 because of a consistent inability to maintain pipette seals with perforated patch solutions with these cells. Nevertheless, in conjunction with the perforated patch and Fluo-4 data from PARP-deficient cells, the results from the PARP-inducible cells provide further support for the conclusion that in lymphocytes, PARP-1 expression is required for both oxidative stress-induced turnover of NAD and oxidative stress-induced gating of TRPM2.

Stable Reconstitution of PARP-deficient DT40 Cells with Human PARP-1 Restores NAD Degradation and TRPM2-dependent Calcium Transients and Currents—The inability to obtain perforated patch clamp data from the PARP-inducible cells left open the possibility that the results from these cells could be the result of PARP-induced alterations in DT40 cell physiology resulting in the reacquisition of Ca^{2+} transients that were independent of TRPM2 gating. To address this issue, we transfected the PARP-deficient DT40 cells with a eukaryotic expression vector driving constitutive PARP-1 expression and isolated several individual stable PARP-1-expressing clones. Evaluation of a panel of clones revealed several with hPARP-1 expression, and a clone that had TRPM2 expression comparable with the PARP-inducible TRPM2 cells, and which was amenable to perforated patch clamp analysis, was chosen for further characterization (designated as "PARP-reconstituted TRPM2" cells; see Fig. 5*A*). Analysis of NAD turnover in the PARP-reconstituted TRPM2 cells demonstrated that, as with the PARP-inducible TRPM2 cells, hPARP1 expression was able to support MNNG- or H_2O_2-induced NAD turnover comparable with that of WT DT40 cells (compare Fig. 5*B* with Fig. 2, *A* and *E*). Furthermore, the reconstituted TRPM2-expressing cells exhibited both MNNG- and H_2O_2-induced TRPM2-dependent calcium transients by Fluo-4 (Fig. 4*D*), and MNNG-induced TRPM2-dependent currents by perforated patch clamp (Fig. 5*E*; again, we were not able to maintain seals in these cells after bath application of H_2O_2). The slower current development in the PARP-reconstituted TRPM2 cells as compared with the DT40-TRPM2 cells was consistently observed, and may be attributable to idiosyncratic differences between cell lines, or that the lower number of channels expressed at the membrane in these cells resulted in reduced Ca^{2+} entry and reduced Ca^{2+}-dependent potentiation of ADPR-dependent TRPM2 gating (18, 23).

DISCUSSION

Here we show that PARP-1 expression is necessary for oxidative stress-induced intracellular NAD turnover and TRPM2-dependent calcium transients and currents in DT40 B lymphocytes. Oxidative stress-induced NAD turnover was completely abolished by genetic ablation of PARP-1 expression, and reconstitution with human PARP-1 fully restored NAD turnover to WT levels. Similarly, oxidative stress-induced TRPM2-dependent Ca^{2+} transients and TRPM2 currents were absent in PARP-1-deficient DT40 cells and were restored after reconstitution of the cells with exogenous PARP-1. In addition, despite the fact that pADPR is produced by PARP and can be found in the cytoplasm (62), only monomeric ADPR, and not pADPR, was able to induce TRPM2-dependent currents. Taken together, these results suggest that the PARP/PARG pathway is directly involved in production of ADP-ribose as an oxidative stress-induced 2nd messenger leading to TRPM2 gating.

A controversial issue in TRPM2 signaling is whether oxidant-induced TRPM2 activation is solely dependent on ADPR or occurs via alternative mechanisms. The lack of perforated patch clamp currents induced by MNNG in PARP-deficient cells suggests that direct oxidant gating is not a major mechanism for TRPM2 activation in our model system. This conclusion is further supported by the lack of TRPM2-dependent increases in cytosolic Ca^{2+} in the PARP-deficient TRPM2 cells, as sustained opening of even a single TRPM2 channel could support sufficient Ca^{2+} current to generate a detectable intracellular Ca^{2+} rise (19, 63–65). The onset of TRPM2-dependent Ca^{2+} transients also consistently occurred subsequent to 50–80% of NAD turnover in DT40-TRPM2 PARP-inducible and PARP-reconstituted TRPM2 cells, suggesting that TRPM2 gating requires turnover of sufficient NAD to allow adenine nucleotide 2nd messenger accumulation. Although Ca^{2+} transients can be influenced by alterations in Ca^{2+} entry or export mechanisms, because individual TRPM2 channels have a known dose-response relationship for ADP-ribose, and our

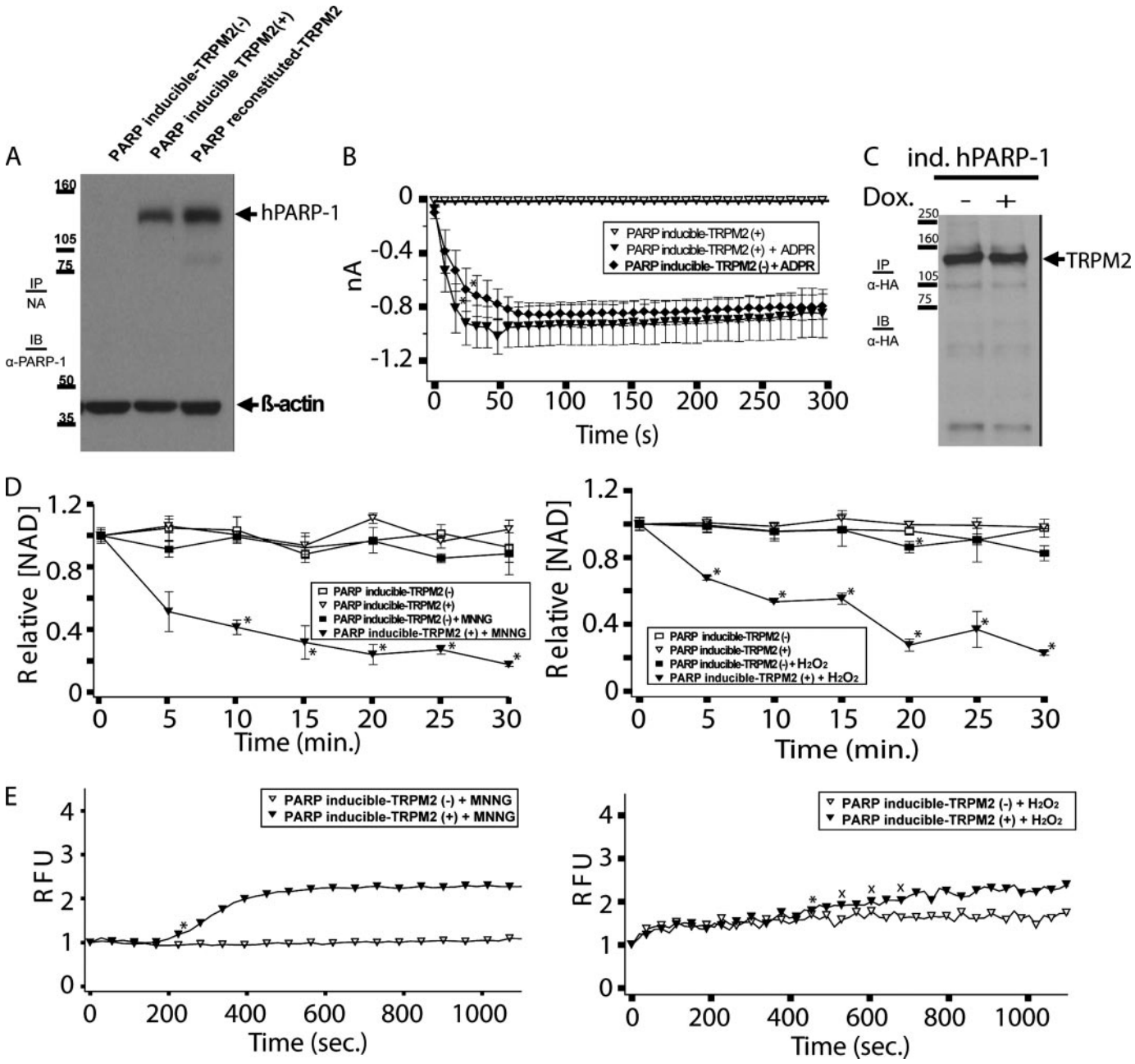

FIGURE 4. **Inducible reconstitution of PARP-deficient DT40 cells with human PARP-1 restores oxidative stress-dependent NAD turnover and TRPM2-dependent Ca^{2+} transients.** *A,* PARP inducible-TRPM2 cells were either left untreated (−) or treated with 1 μg/ml doxycycline (+) to induce hPARP-1 expression. 50 μg of protein from the untreated and treated cells were separated by SDS-PAGE, and analyzed by Western immunoblotting (*IB*) along with PARP reconstituted-TRPM2 cells with rabbit anti-human PARP-1 polyclonal antibody. *IP,* immunoprecipitated. Note that the antibody we used cross-reacts with chicken PARP, allowing us to make comparisons between cell lines expressing chicken PARP (Fig. 3*A*), or between cell lines expressing human PARP (this figure), but not across these two groups. *B,* PARP inducible-TRPM2 cells show similar ADPR-dependent currents by whole cell patch clamp in the presence or absence of hPARP-1 expression. Cells were patched in the whole cell configuration; when the pipette solution contained 100 μM ADPR, ~1 nA of current developed within 50 s in both untreated and doxycycline-treated (1 μg/ml) cells, followed by an extended plateau characteristic of TRPM2, as indicated. *Asterisks* indicate a p value of ≤0.05 from the ADPR-free control. All subsequent points differ from the control with a p value of ≤0.05. Following application of ADPR, the uninduced and induced cells produced TRPM2-dependent whole cell currents that were statistically indistinguishable from one another. *C,* PARP inducible-TRPM2 cells were either left untreated or treated with 1 μg/ml doxycycline. HA-tagged TRPM2 was immunoprecipitated with anti-HA antibody from 500 μg of protein and analyzed by Western immunoblotting. *D,* NAD turnover in PARP-inducible TRPM2 cells requires induction of hPARP1 expression, as indicated. *Asterisks* indicate a p value of ≤0.001 as compared with the untreated controls. *E,* PARP-inducible TRPM2 cells show oxidative stress-induced Ca^{2+} transients, as indicated. PARP-inducible TRPM2 cells were either left untreated or treated with 1 μg/ml doxycycline, and were subsequently treated with 500 μM MNNG or H_2O_2 or left untreated, and intracellular Ca^{2+} was monitored using Fluo-4. *Asterisks* indicate a p value of ≤0.05 from untreated PARP-inducible TRPM2 (−). All subsequent points differ from the uninduced trace with a p value of ≤0.05 except where indicated with an *X*.

whole cell patch analyses demonstrate the presence of sufficient gateable TRPM2 channels to produce current magnitudes in the range of 500 picoamperes in response to saturating [ADPR], the lack of detectable current development in the PARP-deficient cells under perforated patch clamp is most simply explained by a deficiency in ADPR accumulation. If the dose response for ADPR-induced TRPM2 gating in intact DT40 cells is comparable with that measured by whole cell patch clamp in

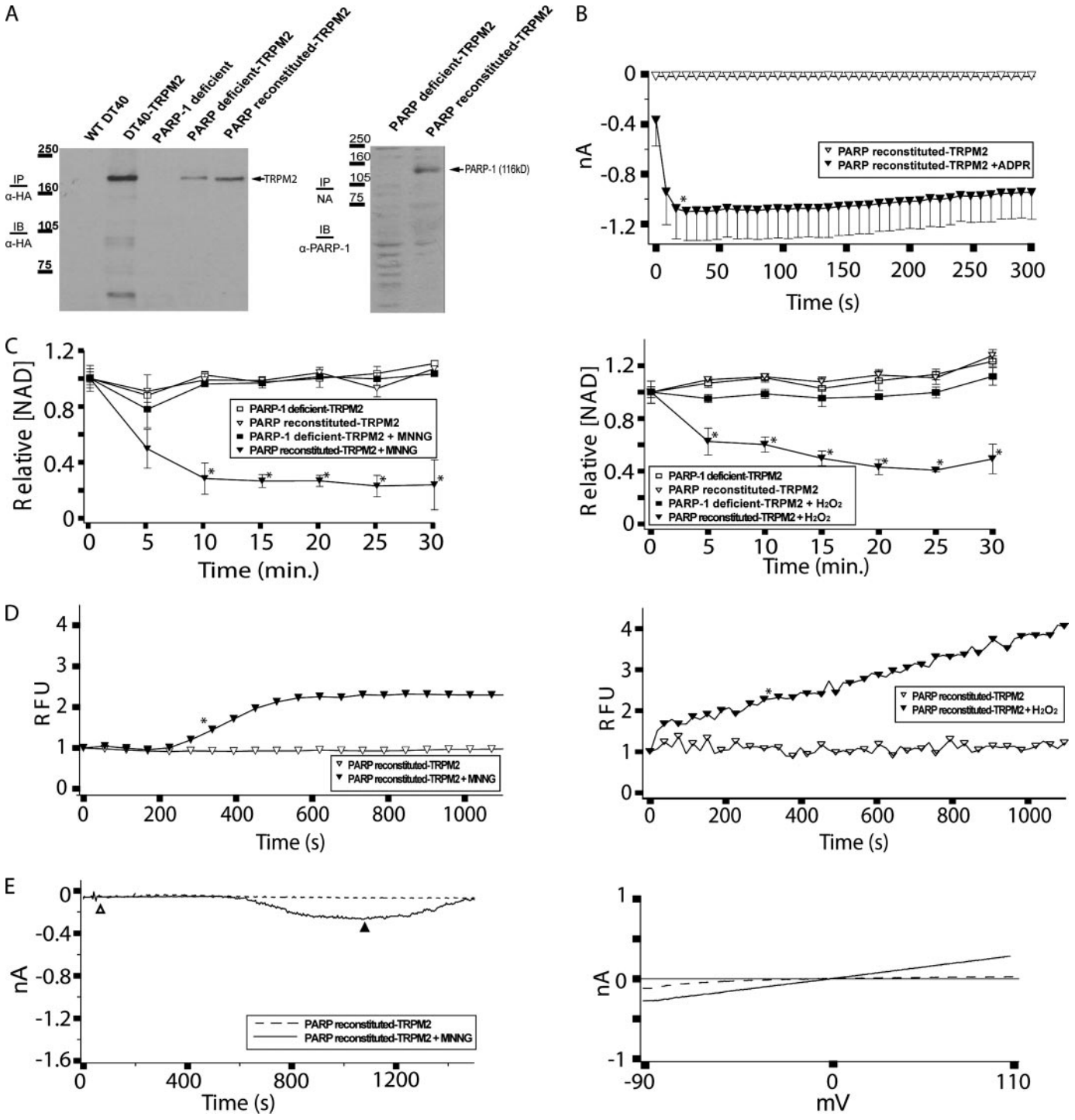

FIGURE 5. **Reconstitution of PARP-deficient DT40 cells with human PARP-1 restores oxidative stress-dependent NAD turnover and TRPM2-dependent Ca^{2+} transients and currents.** *A, left panel,* expression of TRPM2 in DT40-TRPM2, PAR-deficient TRPM2 and PARP-reconstituted TRPM2 cells. HA-tagged TRPM2 was immunoprecipitated (*IP*) from 500 μg of protein extracted from each cell type with mouse anti-HA, run on an SDS-polyacrylamide gel, and immunoblotted (*IB*) with the same antibody. Note: the first 4 lanes of this gel are the same as in Fig. 3*A* and are provided for comparison purposes. *Right panel*: PARP-deficient TRPM2 and PARP-reconstituted TRPM2 cells were lysed, and 50 μg of protein was run in each lane of an SDS-polyacrylamide gel. Rabbit anti-human PARP-1 polyclonal antibody was used for immunoblotting of PARP-1. *B*, PARP-reconstituted TRPM2 cells show ADPR-dependent currents by whole cell patch clamp. PARP-reconstituted TRPM2 cells were patched in the whole cell configuration; when the pipette solution contained 100 μM ADPR, ~1 nA of current developed within 50 s, followed by an extended plateau characteristic of TRPM2, as indicated. *Asterisks* indicate a p value of $\leq$0.05 from the ADPR-free control recording. All subsequent points differ from the control with a p value of $\leq$0.05. *C,* NAD turnover in PARP-reconstituted TRPM2 cells. NAD turnover was assayed in PARP-deficient TRPM2 cells and PARP-reconstituted TRPM2 cells without and with application of 100 μM MNNG or H_2O_2, as indicated. *Asterisks* indicate a p value of $\leq$0.001 as compared with the untreated controls. *D,* PARP-reconstituted TRPM2 cells show oxidative stress-induced Ca^{2+} transients. PARP-reconstituted TRPM2 cells were left untreated or were treated with 500 μM MNNG or H_2O_2, and intracellular Ca^{2+} was monitored using Fluo-4, as indicated. *Asterisks* indicate a p value of $\leq$0.05 from the untreated control. All subsequent points also differ from the control with a p value of $\leq$0.05. *E,* PARP-reconstituted TRPM2 cells show oxidative stress-induced currents. PARP-reconstituted TRPM2 cells were analyzed for MNNG-induced currents using the perforated patch method as described in Fig. 2*E* and under "Experimental Procedures." I/V relationships recorded during the control series (*open triangle*), and the treatment series (*closed triangle*) are shown in the *right panel* as *dashed* or *solid lines*, respectively.

other lymphocyte systems (3), our results suggest that cytosolic free ADPR in the PARP-deficient cells could not be accumulating much above the range of 1–5 μM.

An important issue with PARP-deficient models is that PARP activity is known to have a role in regulating transcription and expression levels of proteins involved in lymphocyte function (66–70). Thus, it is formally possible that PARP-1 is a crucial positive regulator of the expression of enzymes in alternative pathways to adenine nucleotide 2nd messenger formation, as opposed to being directly involved itself. Indeed, the potential relevance of PARP to regulation of transcription is supported by our consistent observation of lower recombinant TRPM2 expression in the PARP-1-deficient background relative to WT or stably reconstituted DT40 cells using the same expression constructs. This observation emphasizes an important advantage of the PARP-deficient DT40 experimental system *versus* PARP-deficient murine models, as we became aware of reduced TRPM2 expression through comparisons among several clonal cell lines. Although an influence of PARP deficiency on alternative mechanisms for adenine nucleotide 2nd messenger production cannot be completely ruled out, the consistency of the results among the WT (support TRPM2 activation by MNNG and H_2O_2), PARP-deficient (do not support TRPM2 activation by MNNG or H_2O_2), and stable and inducibly -reconstituted systems (both recover capacity to support TRPM2 activation by MNNG and H_2O_2) is most parsimoniously explained by a direct role for PARP in the production of ADPR. The generation and analysis of a PARG-deficient system in which TRPM2 gating can be monitored will be required in future studies to more definitively address this question.

An important implication of our results is that PARP-1/PARG pathway activation results not only in nuclear protein ADP-ribosylation but in the accumulation of significant levels of free nuclear and cytosolic ADPR. The concept that free ADPR accumulates after PARP-1/PARG pathway activation has the further implication that physiological effects previously attributed to PARP-1-dependent protein ADP-ribosylation may instead be the result of free ADPR accumulation. Free ADPR has the capacity to influence the function of macro-H2A histones, and thus chromatin physiology. Furthermore, several members of the PARP family contain ADPR-binding macrodomains, and their function may be subject to regulation through soluble free ADPR. Finally, free ADPR may also have a significant influence on cell metabolism, as it is able to act as a competitive inhibitor of NAD binding to the NAD-requiring enzyme glyceraldehyde-3-phosphate dehydrogenase at levels approaching those required to initiate TRPM2 gating (71, 72), and could plausibly act similarly on other NAD-requiring enzymes where NAD binding is mediated primarily by interactions with the ADPR moiety. Thus, accounting for 2nd messenger functions of free ADPR is an important issue for an improved understanding of lymphocyte responses to oxidative stress.

In conclusion, this study describes a genetic approach to analyzing the role of PARP-1 in oxidative stress-induced TRPM2 activation. Our results demonstrate that PARP-1 expression is absolutely required for both oxidative stress-induced NAD turnover and TRPM2 activation, suggesting that the PARP/PARG pathway is the major, if not sole, source of oxidative stress-induced formation of the adenine nucleotide 2nd messenger ADPR. As ADPR produced as a consequence of PARP activation is acting as a TRPM2 gating 2nd messenger, an important implication of these data is that PARP-mediated ADPR accumulation may also act as a 2nd messenger to regulate other physiologically significant events.

REFERENCES

1. Inada, H., Iida, T., and Tominaga, M. (2006) *Biochem. Biophys. Res. Commun.* **350,** 762–767
2. Gasser, A., Bruhn, S., and Guse, A. H. (2006) *J. Biol. Chem.* **281,** 16906–16913
3. Beck, A., Kolisek, M., Bagley, L. A., Fleig, A., and Penner, R. (2006) *FASEB J.* **20,** 962–964
4. Gasser, A., Glassmeier, G., Fliegert, R., Langhorst, M. F., Meinke, S., Hein, D., Kruger, S., Weber, K., Heiner, I., Oppenheimer, N., Schwarz, J. R., and Guse, A. H. (2006) *J. Biol. Chem.* **281,** 2489–2496
5. Kraft, R., Grimm, C., Grosse, K., Hoffmann, A., Sauerbruch, S., Kettenmann, H., Schultz, G., and Harteneck, C. (2004) *Am. J. Physiol.* **286,** C129–C137
6. Zhang, W., Hirschler-Laszkiewicz, I., Tong, Q., Conrad, K., Sun, S. C., Penn, L., Barber, D. L., Stahl, R., Carey, D. J., Cheung, J. Y., and Miller, B. A. (2006) *Am. J. Physiol.* **290,** C1146–D1159
7. Heiner, I., Eisfeld, J., Warnstedt, M., Radukina, N., Jungling, E., and Luckhoff, A. (2006) *Biochem. J.* **398,** 225–232
8. Sano, Y., Inamura, K., Miyake, A., Mochizuki, S., Yokoi, H., Matsushime, H., and Furuichi, K. (2001) *Science* **293,** 1327–1330
9. Hecquet, C. M., Ahmmed, G. U., Vogel, S. M., and Malik, A. B. (2007) *Circ. Res.* **102,** 275–277
10. Fliegert, R., Gasser, A., and Guse, A. H. (2007) *Biochem. Soc. Trans.* **35,** 109–114
11. Grubisha, O., Rafty, L. A., Takanishi, C. L., Xu, X., Tong, L., Perraud, A. L., Scharenberg, A. M., and Denu, J. M. (2006) *J. Biol. Chem.* **281,** 14057–14065
12. Perraud, A. L., Takanishi, C. L., Shen, B., Kang, S., Smith, M. K., Schmitz, C., Knowles, H. M., Ferraris, D., Li, W., Zhang, J., Stoddard, B. L., and Scharenberg, A. M. (2005) *J. Biol. Chem.* **280,** 6138–6148
13. Kuhn, F. J., Heiner, I., and Luckhoff, A. (2005) *Pfluegers Arch.* **451,** 212–219
14. Kolisek, M., Beck, A., Fleig, A., and Penner, R. (2005) *Mol. Cell* **18,** 61–69
15. Wehage, E., Eisfeld, J., Heiner, I., Jungling, E., Zitt, C., and Luckhoff, A. (2002) *J. Biol. Chem.* **277,** 23150–23156
16. Naziroglu, M. (2007) *Neurochem. Res.* **32,** 1990–2001
17. Ishii, M., Shimizu, S., Hara, Y., Hagiwara, T., Miyazaki, A., Mori, Y., and Kiuchi, Y. (2006) *Cell Calcium* **39,** 487–494
18. Starkus, J., Beck, A., Fleig, A., and Penner, R. (2007) *J. Gen. Physiol.* **130,** 427–440
19. Perraud, A. L., Fleig, A., Dunn, C. A., Bagley, L. A., Launay, P., Schmitz, C., Stokes, A. J., Zhu, Q., Bessman, M. J., Penner, R., Kinet, J. P., and Scharenberg, A. M. (2001) *Nature* **411,** 595–599
20. Kuhn, F. J., and Luckhoff, A. (2004) *J. Biol. Chem.* **279,** 46431–46437
21. Massullo, P., Sumoza-Toledo, A., Bhagat, H., and Partida-Sanchez, S. (2006) *Semin. Cell Dev. Biol.* **17,** 654–666
22. Tong, Q., Zhang, W., Conrad, K., Mostoller, K., Cheung, J. Y., Peterson, B. Z., and Miller, B. A. (2006) *J. Biol. Chem.* **281,** 9076–9085
23. McHugh, D., Flemming, R., Xu, S. Z., Perraud, A. L., and Beech, D. J. (2003) *J. Biol. Chem.* **278,** 11002–11006
24. Lee, H. C. (2004) *Curr. Mol. Med.* **4,** 227–237
25. Lee, H. C. (2005) *J. Biol. Chem.* **280,** 33693–33696
26. Moreschi, I., Bruzzone, S., Bodrato, N., Usai, C., Guida, L., Nicholas, R. A., Kassack, M. U., Zocchi, E., and De Flora, A. (2007) *Cell Calcium* **43,** 344–355
27. Billington, R. A., and Genazzani, A. A. (2007) *Cell Calcium* **41,** 505–511
28. Singaravelu, K., and Deitmer, J. W. (2006) *Cell Calcium* **39,** 143–153
29. Moreschi, I., Bruzzone, S., Nicholas, R. A., Fruscione, F., Sturla, L., Benvenuto, F., Usai, C., Meis, S., Kassack, M. U., Zocchi, E., and De Flora, A. (2006) *J. Biol. Chem.* **281,** 31419–31429

30. Kawamura, H., Aswad, F., Minagawa, M., Malone, K., Kaslow, H., Koch-Nolte, F., Schott, W. H., Leiter, E. H., and Dennert, G. (2005) *J. Immunol.* **174,** 1971–1979
31. Broetto-Biazon, A. C., Bracht, F., de Sa-Nakanishi, A. B., Lopez, C. H., Constantin, J., Kelmer-Bracht, A. M., and Bracht, A. (2008) *Mol. Cell. Biochem.* **307,** 41–50
32. Fonfria, E., Marshall, I. C., Benham, C. D., Boyfield, I., Brown, J. D., Hill, K., Hughes, J. P., Skaper, S. D., and McNulty, S. (2004) *Br. J. Pharmacol.* **143,** 186–192
33. Yang, K. T., Chang, W. L., Yang, P. C., Chien, C. L., Lai, M. S., Su, M. J., and Wu, M. L. (2006) *Cell Death Differ.* **13,** 1815–1826
34. Koch-Nolte, F., and Haag, F. (1997) *Adv. Exp. Med. Biol.* **419,** 1–13
35. Ruf, A., de Murcia, G., and Schulz, G. E. (1998) *Biochemistry* **37,** 3893–3900
36. Knight, Z. A., and Shokat, K. M. (2005) *Chem. Biol.* **12,** 621–637
37. Shall, S., and de Murcia, G. (2000) *Mutat. Res.* **460,** 1–15
38. Ame, J. C., Spenlehauer, C., and de Murcia, G. (2004) *Bioessays* **26,** 882–893
39. Menissier de Murcia, J., Ricoul, M., Tartier, L., Niedergang, C., Huber, A., Dantzer, F., Schreiber, V., Ame, J. C., Dierich, A., LeMeur, M., Sabatier, L., Chambon, P., and de Murcia, G. (2003) *EMBO J.* **22,** 2255–2263
40. Buerstedde, J. M., and Takeda, S. (1991) *Cell* **67,** 179–188
41. Lahti, J. M. (1999) *Methods* **17,** 305–312
42. Alinikula, J., Lassila, O., and Nera, K. P. (2006) *Subcell. Biochem.* **40,** 189–205
43. Shinohara, H., and Kurosaki, T. (2006) *Subcell. Biochem.* **40,** 145–187
44. Rainey, M. D., Zachos, G., and Gillespie, D. A. (2006) *Subcell. Biochem.* **40,** 107–117
45. Okada, M., Hori, T., and Fukagawa, T. (2006) *Subcell. Biochem.* **40,** 91–106
46. Caldwell, R. B., and Kierzek, A. M. (2006) *Subcell. Biochem.* **40,** 25–37
47. Hochegger, H., Dejsuphong, D., Fukushima, T., Morrison, C., Sonoda, E., Schreiber, V., Zhao, G. Y., Saberi, A., Masutani, M., Adachi, N., Koyama, H., de Murcia, G., and Takeda, S. (2006) *EMBO J.* **25,** 1305–1314
48. Song, Y., Buelow, B., Perraud, A. L., and Scharenberg, A. M. (2007) *J. Biomol. Screen.* **13,** 54–61
49. Hillyard, D., Rechsteiner, M., Manlapaz-Ramos, P., Imperial, J. S., Cruz, L. J., and Olivera, B. M. (1981) *J. Biol. Chem.* **256,** 8491–8497
50. Hillyard, D., Rechsteiner, M. C., and Olivera, B. M. (1973) *J. Cell. Physiol.* **82,** 165–179
51. Rechsteiner, M., Hillyard, D., and Olivera, B. M. (1976) *J. Cell. Physiol.* **88,** 207–217
52. Diefenbach, J., and Burkle, A. (2005) *Cell Mol. Life Sci.* **62,** 721–730
53. Hour, T. C., Shiau, S. Y., and Lin, J. K. (1999) *Toxicol. Lett.* **110,** 191–202
54. Niknahad, H., and O'Brien, P. J. (1995) *Xenobiotica* **25,** 91–101
55. Han, W., Takano, T., He, J., Ding, J., Gao, S., Noda, C., Yanagi, S., and Yamamura, H. (2001) *Antioxid. Redox Signal.* **3,** 1065–1073
56. Strosznajder, R. P., Jesko, H., and Adamczyk, A. (2005) *J. Physiol. Pharmacol.* **56,** Suppl. 4, 209–213
57. Kun, E., Kirsten, E., Mendeleyev, J., and Ordahl, C. P. (2004) *Biochemistry* **43,** 210–216
58. Inamura, K., Sano, Y., Mochizuki, S., Yokoi, H., Miyake, A., Nozawa, K., Kitada, C., Matsushime, H., and Furuichi, K. (2003) *J. Membr. Biol.* **191,** 201–207
59. Heiner, I., Radukina, N., Eisfeld, J., Kuhn, F., and Luckhoff, A. (2005) *Naunyn Schmiedebergs Arch. Pharmacol.* **371,** 325–333
60. Song, Y., Buelow, B., Perraud, A. L., and Scharenberg, A. M. (2008) *J. Biomol. Screen.* **13,** 54–61
61. Takano, T., Sada, K., and Yamamura, H. (2002) *Antioxid. Redox Signal.* **4,** 533–541
62. Yu, S. W., Andrabi, S. A., Wang, H., Kim, N. S., Poirier, G. G., Dawson, T. M., and Dawson, V. L. (2006) *Proc. Natl. Acad. Sci. U. S. A.* **103,** 18314–18319
63. Parekh, A. B., and Penner, R. (1997) *Physiol. Rev.* **77,** 901–930
64. Lewis, R. S. (2001) *Annu. Rev. Immunol.* **19,** 497–521
65. Cahalan, M. D., Wulff, H., and Chandy, K. G. (2001) *J. Clin. Immunol.* **21,** 235–252
66. Kraus, W. L., and Lis, J. T. (2003) *Cell* **113,** 677–683
67. Ogino, H., Nozaki, T., Gunji, A., Maeda, M., Suzuki, H., Ohta, T., Murakami, Y., Nakagama, H., Sugimura, T., and Masutani, M. (2007) *BMC Genomics* **8,** 41
68. Harnacke, K., Kruhoffer, M., Orntoft, T. F., and Hass, R. (2005) *Eur. J. Cell Biol.* **84,** 885–896
69. Valdor, R., Schreiber, V., Saenz, L., Martinez, T., Munoz-Suano, A., Dominguez-Villar, M., Ramirez, P., Parrilla, P., Aguado, E., Garcia-Cozar, F., and Yelamos, J. (2007) *Mol. Immunol.* **45,** 1863–1871
70. Meder, V. S., Boeglin, M., de Murcia, G., and Schreiber, V. (2005) *J. Cell Sci.* **118,** 211–222
71. Du, X., Matsumura, T., Edelstein, D., Rossetti, L., Zsengeller, Z., Szabo, C., and Brownlee, M. (2003) *J. Clin. Invest.* **112,** 1049–1057
72. Shen, Y. Q., Song, S. Y., and Lin, Z. J. (2002) *Acta Crystallogr. Sect. D Biol. Crystallogr.* **58,** 1287–1297
73. Ferraris, D., Ko, Y. S., Pahutski, T., Ficco, R. P., Serdyuk, L., Alemu, C., Bradford, C., Chiou, T., Hoover, R., Huang, S., Lautar, S., Liang, S., Lin, Q., Lu, M. X., Mooney, M., Morgan, L., Qian, Y., Tran, S., Williams, L. R., Wu, Q. Y., Zhang, J., Zou, Y., and Kalish, V. (2003) *J. Med. Chem.* **46,** 3138–3151
74. Jacobson, M. K., and Jacobson, E. L. (1999) *Trends Biochem. Sci.* **24,** 415–417
75. Ono, T., Kasamatsu, A., Oka, S., and Moss, J. (2006) *Proc. Natl. Acad. Sci. U. S. A.* **103,** 16687–16691
76. Niere, M., Kernstock, S., Koch-Nolte, F., and Ziegler, M. (2008) *Mol. Cell. Biol.* **28,** 814–824
77. Aarhus, R., Graeff, R. M., Dickey, D. M., Walseth, T. F., and Lee, H. C. (1995) *J. Biol. Chem.* **270,** 30327–30333
78. Buck, S. W., Gallo, C. M., and Smith, J. S. (2004) *J. Leukocyte Biol.* **75,** 939–950
79. Denu, J. M. (2003) *Trends Biochem. Sci.* **28,** 41–48
80. Hsiao, S. J., and Smith, S. (2008) *Biochimie* (*Paris*) **90,** 83–92
81. Yeh, T. Y., Sbodio, J. I., and Chi, N. W. (2006) *Biochem. Biophys. Res. Commun.* **350,** 574–579
82. Chang, P., Coughlin, M., and Mitchison, T. J. (2005) *Nat. Cell Biol.* **7,** 1133–1139
83. Compton, D. A. (2005) *Biochem. J.* **391,** e5–6
84. Chang, W., Dynek, J. N., and Smith, S. (2005) *Biochem. J.* **391,** 177–184
85. Goenka, S., Cho, S. H., and Boothby, M. (2007) *J. Biol. Chem.* **282,** 18732–18739
86. Goenka, S., and Boothby, M. (2006) *Proc. Natl. Acad. Sci. U. S. A.* **103,** 4210–4215
87. Aguiar, R. C., Takeyama, K., He, C., Kreinbrink, K., and Shipp, M. A. (2005) *J. Biol. Chem.* **280,** 33756–33765
88. Inoue, T., Hiratsuka, M., Osaki, M., and Oshimura, M. (2007) *Cell Cycle* **6,** 1011–1018
89. Yamamoto, H., Schoonjans, K., and Auwerx, J. (2007) *Mol. Endocrinol.* **21,** 1745–1755
90. Anastasiou, D., and Krek, W. (2006) *Physiology* (*Bethesda*) **21,** 404–410
91. Yang, T., Fu, M., Pestell, R., and Sauve, A. A. (2006) *Trends Endocrinol. Metab.* **17,** 186–191
92. Tang, B. L. (2006) *Neurobiol. Aging* **27,** 501–505
93. Bordone, L., and Guarente, L. (2005) *Nat. Rev. Mol. Cell Biol.* **6,** 298–305
94. Nakamura, Y., Ogura, M., Tanaka, D., and Inagaki, N. (2008) *Biochem. Biophys. Res. Commun.* **366,** 174–179
95. Lombard, D. B., Alt, F. W., Cheng, H. L., Bunkenborg, J., Streeper, R. S., Mostoslavsky, R., Kim, J., Yancopoulos, G., Valenzuela, D., Murphy, A., Yang, Y., Chen, Y., Hirschey, M. D., Bronson, R. T., Haigis, M., Guarente, L. P., Farese, R. V., Jr., Weissman, S., Verdin, E., and Schwer, B. (2007) *Mol. Cell. Biol.* **27,** 8807–8814
96. Michishita, E., Park, J. Y., Burneskis, J. M., Barrett, J. C., and Horikawa, I. (2005) *Mol. Biol. Cell* **16,** 4623–4635
97. Allison, S. J., and Milner, J. (2007) *Cell Cycle* **6,** 2669–2677
98. Yang, H., Yang, T., Baur, J. A., Perez, E., Matsui, T., Carmona, J. J., Lamming, D. W., Souza-Pinto, N. C., Bohr, V. A., Rosenzweig, A., de Cabo, R., Sauve, A. A., and Sinclair, D. A. (2007) *Cell* **130,** 1095–1107
99. Scher, M. B., Vaquero, A., and Reinberg, D. (2007) *Genes Dev.* **21,** 920–928

100. Shi, T., Wang, F., Stieren, E., and Tong, Q. (2005) *J. Biol. Chem.* **280,** 13560–13567
101. Onyango, P., Celic, I., McCaffery, J. M., Boeke, J. D., and Feinberg, A. P. (2002) *Proc. Natl. Acad. Sci. U. S. A.* **99,** 13653–13658
102. Schwer, B., North, B. J., Frye, R. A., Ott, M., and Verdin, E. (2002) *J. Cell Biol.* **158,** 647–657
103. Ahuja, N., Schwer, B., Carobbio, S., Waltregny, D., North, B. J., Castronovo, V., Maechler, P., and Verdin, E. (2007) *J. Biol. Chem.* **282,** 33583–33592
104. Haigis, M. C., Mostoslavsky, R., Haigis, K. M., Fahie, K., Christodoulou, D. C., Murphy, A. J., Valenzuela, D. M., Yancopoulos, G. D., Karow, M., Blander, G., Wolberger, C., Prolla, T. A., Weindruch, R., Alt, F. W., and Guarente, L. (2006) *Cell* **126,** 941–954
105. Mostoslavsky, R., Chua, K. F., Lombard, D. B., Pang, W. W., Fischer, M. R., Gellon, L., Liu, P., Mostoslavsky, G., Franco, S., Murphy, M. M., Mills, K. D., Patel, P., Hsu, J. T., Hong, A. L., Ford, E., Cheng, H. L., Kennedy, C., Nunez, N., Bronson, R., Frendewey, D., Auerbach, W., Valenzuela, D., Karow, M., Hottiger, M. O., Hursting, S., Barrett, J. C., Guarente, L., Mulligan, R., Demple, B., Yancopoulos, G. D., and Alt, F. W. (2006) *Cell* **124,** 315–329
106. Liszt, G., Ford, E., Kurtev, M., and Guarente, L. (2005) *J. Biol. Chem.* **280,** 21313–21320
107. Bentle, M. S., Reinicke, K. E., Bey, E. A., Spitz, D. R., and Boothman, D. A. (2006) *J. Biol. Chem.* **281,** 33684–33696